Flood monitoring over the Mackenzie River Basin using passive microwave data

Marouane Temimi *, Robert Leconte, Francois Brissette, Naira Chaouch

École de Technologie Supérieure, Montreal, Canada Montreal, Québec, Canada

Abstract

Flooding over the Mackenzie River Basin, which is situated in northwestern Canada, is a complex and rapid process. This process is mainly controlled by the occurrence of ice jams. Flood forecasting is of very important in mitigating social and economic damage. This study investigates the potential of a rating curve model for flood forecasting. The proposed approach is based on the use of a Water Surface Fraction derived from SSM/I passive microwave images and discharge observations. The rating curve model is based on an existing correlation between flooded areas and measured discharge. However, a time lag can be observed between these two variables. Thus, the rating curve model has been modified by the introduction of a lag term that could vary depending on the flooding intensity and the features of the basin. Hence, the lag term is computed dynamically using a cross-correlation function between Water Surface Fraction values which are derived from SSM/I observations and the discharge vectors. The rating curve model is based on two empirical parameters that depend on the site features, which vary in both space and time. To overcome this dependency, the rating curve model was linked to a Kalman filter in order to dynamically estimate the empirical parameters according to the forecasting errors encountered at each time step. With the Kalman filter, the dynamic rating curve model continuously readjusts its parameters to satisfy the non-stationary behavior of hydrological processes. The model is thus sufficiently flexible and adapted to various conditions. Simulations were carried out over the Mackenzie River Basin (1.8 million km^2) during the summers of 1998 and 1999. NOAA-AVHRR images were used to validate the forecast WSF values. The predicted flooded areas agree well with those derived from the NOAA-AVHRR images. Further simulations were carried out from 1992 to 2000 using the rating curve model to predict discharge at a downstream location. Even though an interannual variability of the water surface fractions was observed over the PAD area, the modified model was sufficiently flexible to be readjusted and to reproduce satisfactory results. This implies that a combination of passive microwave data and discharge observations presents an interesting potential in flood and discharge prediction.
© 2005 Elsevier Inc. All rights reserved.

Keywords: Flood monitoring; Passive microwave data; Discharge observations; Rating curve; Kalman filter

1. Introduction

This work is part of the Mackenzie GEWEX Study, MAGS. MAGS is the Canadian contribution to the GEWEX international program. The main objective of the MAGS project is to provide an understanding of the hydrological and climatological processes occurring within the Mackenzie River Basin (MRB), in northwestern Canada. The estimation of the Water Surface Fraction (WSF) over a basin is of great importance for modeling hydrological and climatological processes. WSF is a useful indicator of water storage fluctuations and a crucial parameter in flood monitoring as it indicates the variation of flooded areas in both space and time. However, hydrological processes can vary rapidly. Moreover, ice jamming significantly controls the occurrence of flooding in northern climates. To predict the evolution of these processes, a real-time forecasting of the WSF is needed. Remote sensing presents an interesting potential for flood prediction.

Usually, the WSF is estimated using a combination of one or multiple frequencies at different polarizations. Fily et al. (2003) proposed an approach to estimate WSF based

* Corresponding author. Tel.: +1 514 396 8800x7690; fax: +1 514 396 8584.

E-mail address: Marouane.temimi.1@ens.etsmtl.ca (M. Temimi).

on the ratio ($e_{soil} - e_{dry\ soil}/e_{wet\ soil} - e_{dry\ soil}$), where e_{soil}, $e_{dry\ soil}$, $e_{wet\ soil}$ are the emissivities of the observed, dry and wet soils, respectively. The emissivity, in the work of Fily et al. (2003), was estimated from a relationship established between 19 and 37 GHz brightness temperatures vertically and horizontally polarized, provided by SSM/I sensor. Tanaka et al. (2003) tested two different methods. The first was based on the use of the SSM/I 37 GHz channel as a single frequency. The 37 GHz horizontally polarized channel was considered optimal as it has a smaller effective field of view (EFOV) and a horizontal polarization that presents a greater contrast between water and dry soil. The second method was based on the use of a polarization difference at the 37 GHz frequency level, also using SSM/I data. Both of these methods showed a good agreement with WSF derived from NOAA-AVHRR data. SSM/I data were used also by Jin (1999) to compute a flooding index (FI), defined as the difference between vertically polarized brightness temperatures measured at 37 and 85 GHz frequencies, respectively. The FI was compared to predetermined threshold F_0 indicating flood detection.

A Basin Wetness Index (BWI) was suggested by (Basist et al., 1998). The BWI is based on the correlation between the emissivity decrease and the presence of water at or near the soil surface which affects the brightness temperature differences measured at 19, 37 and 85 GHz. The moisture in the soil reduces its emissivity and affects the differences between emissivities estimated at different frequencies. Furthermore, this index allows the calculation of the WSF, which is a potential indicator of water storage within the upper soil layer. In this work, a particular interest has been given to the wetness index proposed by Basist et al. (1998). This index was selected because of its simplicity and the availability of data allowing its application.

This work aims to provide a real-time forecast of the WSF over the Mackenzie River Basin, which is situated in northwestern Canada (Fig. 1), using passive microwave data. The method is based on a rating curve relating discharge measurements to water extent derived from microwave data. In addition, a Kalman filter has been used to update the empirical parameters of the rating curve model. Section 2 of this article will discuss firstly the potential of passive microwave to estimate WSF over large watersheds and secondly the use of the Kalman filter to take into account the temporal variability of the empirical parameters of the rating curve model. Finally, the results of the application of the proposed method will be presented in Section 3.

2. Methodology

2.1. Estimation of the water surface extent using passive microwave data

Basist et al. (1998) proposed an approach based on the correlation between the decrease of emissivity and the brightness temperature differences. The gradual change in
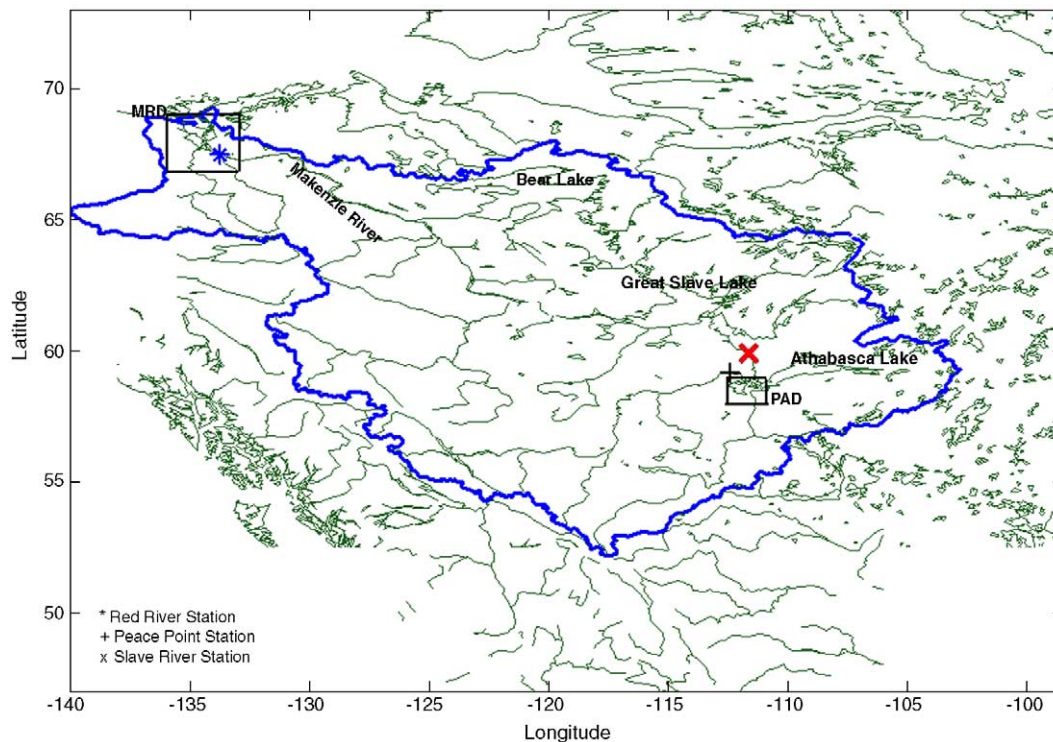

Fig. 1. The Mackenzie River Basin.

space of the land emissivity depends on the frequency and the amount of water at and/or near the surface. They defined a Basin Wetness Index (BWI), which is sensitive to liquid water within the satellite field of view (FOV). This index was estimated by a linear combination of brightness temperatures remotely sensed by SSM/I in the 19, 37 and 85 GHz vertically polarized frequencies. Thus, the BWI and WSF derived from this index are written as:

$$BWI = \beta_0[T_b(\nu_2) - T_b(\nu_1)] + \beta_1[T_b(\nu_3) - T_b(\nu_2)] \qquad (1)$$

$$WSF = \frac{1 - \dfrac{T_{b(19V)}}{\dfrac{1}{\varepsilon_0}\left(T_{b(19V)} + BWI\right)}}{0.33} \qquad (2)$$

where $T_b(\nu_1)$, $T_b(\nu_2)$ and $T_b(\nu_3)$ are brightness temperatures measured by the SSM/I at 19, 37 and 85 GHz, respectively. β_0 and β_1 are two empirical parameters that account for the non-linear decrease of the emissivity with moisture at high frequencies. In addition, these parameters account for the mismatching FOVs, which vary from 60 km at 19 GHz to 15 km at 85 GHz (Basist et al., 2001; Tanaka et al., 2003). This index allows the calculation of the WSF (Eq. (2)).b, which is a potential indicator of water storage within the upper soil layer. Refer to Basist et al. (1998) for a complete description of the procedure to calculate the BWI.

According to Basist et al. (1998), empirical parameters, β_0 and β_1, are constant for both space and time. Williams et al. (2000) have proposed calibrating them based on surface types. Hence, a preliminary classification exercise was required in their study to identify surface types. Several surface types need to be defined in order to improve the reliability of the approach (Williams et al., 2000).

The temporal evolution of the vegetation and surface conditions should have an effect on the emission process and consequently on the relationship between the BWI and the brightness temperature differences. The vegetation growth during the summer season decreases the portion of soil surface "seen" by a microwave sensor and affects the soil emissivity. However, brightness temperatures are highly affected by the presence of moisture near the soil surface. As a result, the BWI sensitivity to soil moisture should vary during the summer season. Therefore, the relationship between the emissivity reduction, due to wetness, and the brightness temperature differences which define the BWI, needs to be readjusted over time. It is essential to take into account the evolution of the vegetation cover in order to improve the index sensitivity to wet surfaces.

In order to overcome the classification step and account for the temporal evolution of the vegetation cover, it is suggested to dynamically update the parameters of the BWI at the reception of each new image and on a pixel per pixel basis. Hence, a mobile window was programmed to scan the image. The window width was fixed at 5 pixels. Considering the SSM/I image resolution, the total width of the window is 125 km. Considering that it is the trend of the parameters that will be used to estimate BWI and FWS, the size of the mobile window does not seem to be crucial. At the reception of each new image, the empirical parameters are estimated for the central pixel of the mobile window, allowing the temporal variation of these parameters to be assessed. The results obtained will be used in this study as an estimation of the WSF. It is expected that this dynamic readjustment will improve the BWI, and therefore the WSF sensitivity to the liquid water on the soil surface.

SSM/I data, used in this study, were extracted from the National Snow and Ice Data Center (NSIDC) database (Armstrong et al., 1994). The resolution of the SSM/I imported images (ascending mode) is 25 km for 19 and 37 GHz, and 12.5 km for 85 GHz, which are mapped in polar Azimuthal Equal-Area grids. The 19, 37 and 85 GHz vertically polarized frequency channels of the SSM/I sensor were used to estimate the WSF by a linear combination of these frequencies.

2.2. The rating curve formula

Several studies have proven that there is a strong correlation between hydrological parameters, discharge or stage, and flooded areas (Frazier et al., 2003; Mosley, 1983; Smith et al., 1996; Vorosmarty et al., 1996). Smith et al. (1995) used the measurements of flooded areas derived from ERS-1 SAR images to estimate the discharge of a glacial river in British Columbia. Their approach was based on a rating curve model written as:

$$W = a\,Q^b \qquad (3)$$

where W is the effective width which is defined as the total water surface area divided by the length of the main drainage channel. Q is the measured discharge and "a" and "b" are two empirical parameters. Despite its simplicity and interesting potential, particularly over large watersheds, the main problem of using this simple empirical relationship in flood forecasting is its dependency on surface type conditions. The empirical parameters vary significantly from one site to another. Moreover, the temporal evolution of the surface conditions in the basin suggests that these parameters may well vary with time. It is interesting to analyze the potential of this model for water surface extent prediction using passive microwave data and discharge measurements. The problem of spatial and temporal constancy of the classic power law model parameters will be particularly examined.

The relationship between flooded areas and discharge in northern climates depends largely on the occurrence of ice jams in the main channel of rivers. Moreover, the presence of vegetation and semi-active zones that join the hydrological network only during flooding can also control the
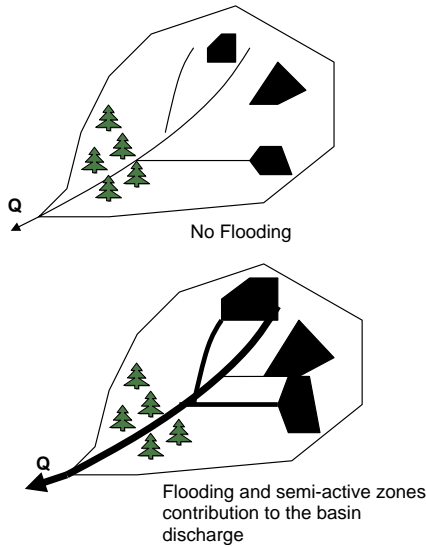
Fig. 2. Discharge measured at the basin outlet is used as a proxy for temporal variation in WSF derived from passive microwave data.

relationship between discharge and water body extent. Generally, the flooded area increases with increasing discharge (Fig. 2). This relationship leads to a rating curve model relating the flooded area to the discharge, written as:

$$\text{WSF}(t) = a. \, Q^b(t) \tag{4}$$

where WSF is the Water Surface Fraction, Q is the measured discharge, and a and b are two empirical parameters. Generally, these empirical parameters are determined by a linearization of Eq. (4). The power law model (Eq. (4)) was selected because of its simplicity and the availability of the parameters required for its imple-

mentation. The easy availability of the parameters represents a great advantage for estimating the water body extent. The relationship between the flow and the WSF is expected to vary with time. Fig. 3 shows the relationship between the measured flow and the estimated WSF over the Mackenzie River Basin outlet, during the summer of 1998. This figure shows that there are two sets of data, one for the flooding phase, and a second set for the recession phase. These different data sets will affect the estimation accuracy of the parameters of the rating curve model. Thus, the estimation of the parameters should account for the changing relationship between the flow and the WSF.

The rating curve relation under its classical equation implies a systematic synchronism between the inundation and discharge curves. However, a lag time is generally observed between the flow peak and maximum water surface area over large watersheds (Sippel et al., 1998). Furthermore, the river stage can increase while the flooded area decreases (Kruus et al., 1981). These phenomena were also observed in the Mackenzie River Basin. Consequently, the assumption of a systematic synchronism is therefore not realistic. In order to account for the occurrence of a time lag, an additional term was introduced into the rating curve formula. Thus, the model is now written as:

$$\text{WSF}(t) = a. \, Q^b \, (t + \text{d}.\Delta\text{t}) \tag{5}$$

where "d.Δt" is a time lag between the discharge and the flooded area. Many factors are likely to generate a time lag between flows and the flooded area: 1) the flow measurement location in the basin; 2) the river morphology; 3) ice jamming, and 4) vegetation density in the flooded area. Furthermore, three situations can be encountered: the lag parameter can be positive if the peak flow occurs after the peak flooded area; it is equal to zero if the two maxima
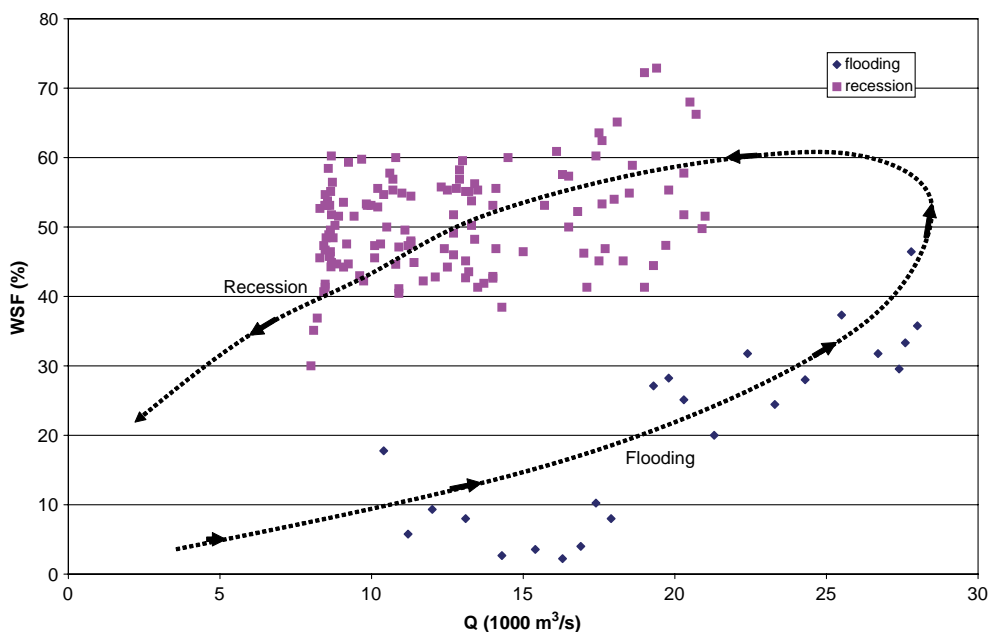

Fig. 3. The relationship between measured flow and WSF estimated over the Mackenzie River Basin Outlet, during the summer of 1998.

coincide, and finally, if the discharge peak precedes the maximum flooded extent, the time lag will be negative. The model is thus sufficiently flexible and adaptable to those conditions.

Theoretically, the time lag term will maximize the value of the cross-correlation function between the discharge and flooded area curves. This lag depends on the site morphology, and can vary even over the same site during the summer particularly if the site experiences multiple flood events. Hence, a window is programmed to follow data acquisition, extract the last ten values of the discharge and flooded area, and estimate the lag term using the cross-correlation function.

The dependency on the river morphology is the main weakness of the classic rating curve approach. This model, and therefore its empirical parameters, cannot be easily extrapolated from one site to another, even in the case of braided rivers. Moreover, the occurrence of ice jams can affect the relationship between the observed discharge and the estimated WSF, thus suggesting an update of the empirical parameters of the rating curve, which were considered as constant according to the classical formula of the model. Hence, the variability of the empirical parameters of the model presents temporal and spatial components. To overcome these weaknesses, the rating curve model can be related to a Kalman filter in order to dynamically identify its empirical parameters according to the forecasting errors compared at each time step. Using the Kalman filter, the dynamic rating curve model will continuously readjust its parameters to satisfy the non-stationary behavior of the hydrological phenomenon.

The parameter constancy and the systematic synchronism between the flooded area and the discharge are two weaknesses that inhibit the use of the rating curve model for flood forecasting. By introducing a lag term and relating the classical model formula to the Kalman filter, it is expected that these weaknesses should be overcome. With this dynamic formula, it is expected that the model will present an interesting potential for flood forecasting over large basins, where spatial conditions can vary largely from one site to another. It will also eliminate the classical calibration approach that leads to the estimation of two constant values of the empirical parameters. These parameters will vary with time and space in order to produce, at near real time, the highest correlation between the flooded area and the discharge expressed by the rating curve model.

2.3. Use of the of Kalman filter

The use of the Kalman filter is based on the application of the logarithm to the modified rating curve formula. A linear relationship can be written as:

$$\mathrm{Log}\left(\mathrm{WSF}_{(t)}\right) = \log(a) + (b)\log\left(Q_{(t+\mathrm{d}.\Delta t)}\right) \qquad (6)$$

or

$$Y = AX + B \qquad (7)$$

where: $Y = \mathrm{Log}\,(\mathrm{WSF}(t))$; $X = \log(Q_{(t+\mathrm{d}.\Delta t)})$; A and B are two model parameters.

According to the linear relationship, the rating curve model can be written as a matrix product:

$$Y_t = H_t.A_t \qquad (8)$$

where $Y_t = Y$

$$A_t = \begin{bmatrix} A \\ B \end{bmatrix}$$

$$H_t = \begin{bmatrix} X & 1 \end{bmatrix}.$$

The Kalman filter can therefore be applied to the rating curve model by considering the modeling and observation noises. The state and observation equations will be written as:

$$A_{t+1} = \Phi_t A_t + W_t \qquad (9)$$

$$Y_t = H_t A_t + V_t. \qquad (10)$$

Upon reception of a satellite image (i.e. SSM/I), a WSF is calculated, followed by a readjustment of the parameters of the rating curve model by the Kalman filter. The cross-correlation function evaluates the lag time between the two vectors of observation. Hence, the WSF value will be predicted using updated parameters and an estimated time lag. It is expected that the combination of these two procedures will improve the flood prediction potential of the rating curve model.

3. Application and results

3.1. Study area: the Mackenzie River Basin

The methodology proposed in this work was applied to the Mackenzie River Basin (MRB) (Fig. 1). Going from south to north, the vegetation zones in the Mackenzie Basin vary from prairies to boreal forests to tundra, in the northerly part of the basin. In the western part of the basin, mountains rise up to 3 km, and the lowest zones lie in the northern and central-eastern parts of the basin (Rouse, 2000; Stewart et al., 1998). The Mackenzie Basin contains some of the largest freshwater lakes in the world: Great Bear Lake, Great Slave Lake and Athabasca Lake. These lakes play an important role in water cycle monitoring in the Mackenzie River Basin. Freshwater lakes and distributary channels cover up to 50% of the total Mackenzie Delta area (Burn, 1995).

The water cycle in the MRB is largely affected by the spring snow melt period, during which ice thawing is its major source of freshwater. Similarly, in the Basin's lakes and rivers, the water level rises to its highest level during this period. Consequently, river discharge becomes very significant and many lakes flooded. Note that flooding over the Mackenzie River Basin is largely affected by ice jamming. Marsh and Hey (1989) stated that 33% of lakes

in the Mackenzie Delta can be considered as high-closure lakes. In this case, ice jamming dominates flooding. Thus, these lakes are mainly flooded during the spring melt period, when ice jamming occurs. Over the Peace-Athabasca Delta, Toyra et al. (2002) observed several wetland basins surrounding the delta. The central part of the delta is mainly composed of large and shallow lakes which are connected to Lake Athabasca by several channels. Generally, these wetland basins are not connected to the main channel. However, following the ice break-up, a portions of these basins flood rapidly (Leconte et al., 2001). Hence, flooding in two major deltas of the Mackenzie River Basin, namely, the Mackenzie River Delta and the Peace-Athabasca Delta, depends largely on the spring snow melt period. Furthermore, flooding frequencies in these areas are highly related to their morphology as most of these wetland basins are disconnected, and only join the main river during the spring melt period as a result of ice jams. Therefore, during the spring melt period, these flooded areas include either basins covered by shallow water or wetlands with highly moist soils.

3.2. Approach reliability assessment using 1998 and 1999 data

WSF values over the Mackenzie River Basin were estimated during the summers of 1998 and 1999 on a pixel-per-pixel basis. These estimations were used in this application to carry out offline simulations, and were considered as "true" values to which the predicted WSF were compared. From the daily generated WSF maps, the Peace Athabasca Delta (PAD) and the Mackenzie River delta (MRD) were selected as control sections in order to assess the reliability of the proposed approach (Fig. 1). The PAD

and the MRD have areas of about 4000 and 12 000 km², respectively. The estimated WSF was averaged over each control section in order to apply the proposed methodology. The estimated WSF can be affected by atmospheric conditions, especially during wet seasons (Kerr & Njoku, 1993). However, the flooding effect will dominate the WSF variability as simulations were curried out over two deltas with a high flood potential. The existence of a significant correlation between flooded areas and discharges over these areas is the most important reason for choosing these two deltas for the application of the methodology. Furthermore, the flat topography of these selected deltas reduces the contribution to the satellite signal of high-closure lakes that do not join the main river stem, even during the spring melt period. Moreover, previous studies (Sippel et al., 1992; Vorosmarty et al., 1996) recommended an analysis of the correlation between discharge and floodplain extent within the main stem. The main river stems were included in the selected portions in this study.

River runoff data were provided by two observation sites, the first being at the Arctic Red River (67° 27 N, 133° 44 W), which corresponds to an outflow of almost 95% of the MRB (MacKay et al., 2003), and the second at the Peace River (59°6 N, 112°25 W), for the MRD and PAD, respectively (Fig. 1). The location of these stations is very important with respect to the time lag between discharge and flow measurements. Generally, the observation sites over the Mackenzie Basin allow accurate measurements of river runoff. However, the accuracy is sometimes reduced, especially during the ice-cover and spring melt periods (Stewart et al., 1998). In spite of the ice jam effect which occurs during the spring melt period, discharge measurements provided by these stations are reasonably accurate for the purposes of this study.
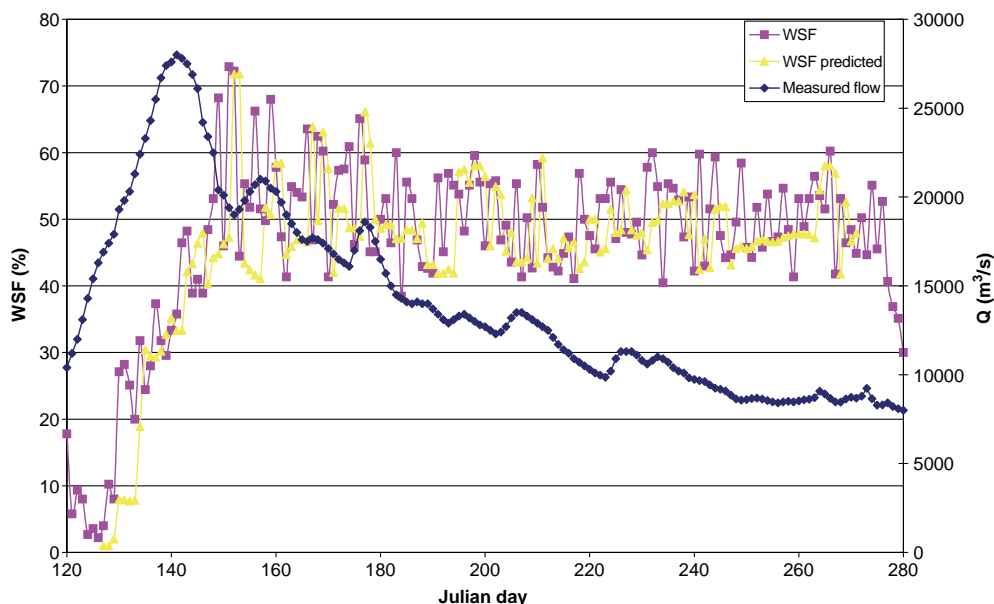

Fig. 4. Predicted and estimated WSF compared to the Mackenzie River at Arctic Red River discharge, over the MRD, during the summer of 1998.
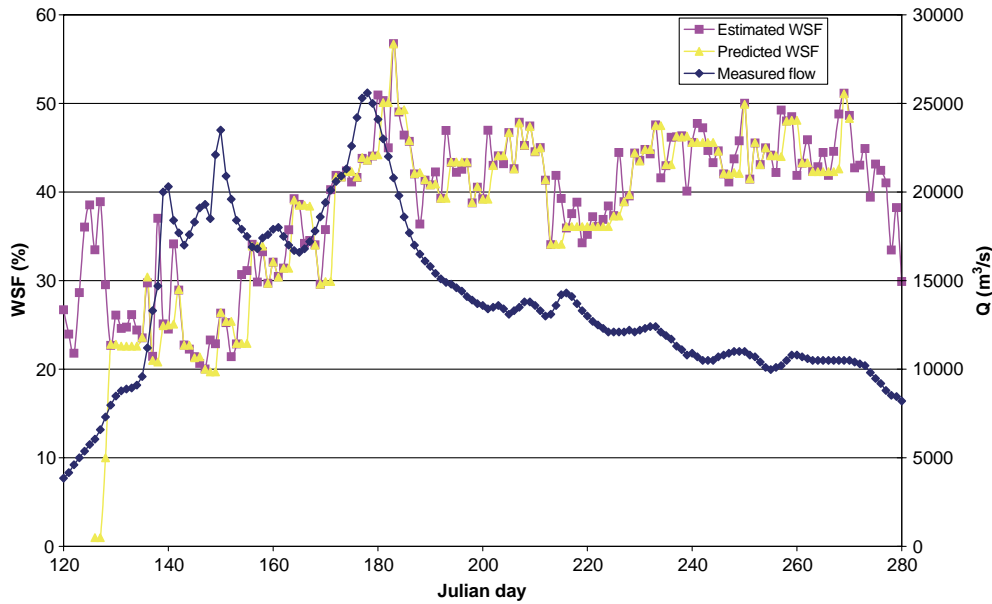
Fig. 5. Predicted and estimated WSF compared to the Mackenzie River discharge, over the MRD, during the summer of 1999.

It is interesting to note that according to the proposed approach, the calibration step of the rating curve model is not needed as the rating curve parameters are adjusted upon the reception of each new WSF value. Therefore, the entire 1998 and 1999 data set was used to carry out the simulations. With two zones and two summer seasons, four flooding events were used to assess the reliability of the approach. Figs. 4–7 illustrate the results obtained with the approach.

Results show a good agreement between the estimated and predicted WSF. For all four flooding events, the rating curve model was able to satisfactorily simulate the trend of the estimated WSF. All analyzed events show an increasing WSF during the spring melt period as ice thawing and

precipitations contribute to extend the WSF over the Mackenzie River Basin. This is followed by a flattening of the curves during the months of June and July, as precipitation and snowmelt are compensated by evaporation and discharge. However, some flooding events can be observed during the summer seasons, with a lower magnitude as compared to those of the spring melt period (Marsh & Hey, 1989). Finally, a decrease of the WSF is noticed as the snowmelt no longer contributes to the hydrological cycle and evaporation plus runoff exceeds precipitation. Furthermore, the predicted WSF for 1998 were higher than those for 1999, over the same area. It is interesting to note that 1998 was 8th wettest year observed in the Mackenzie River Basin
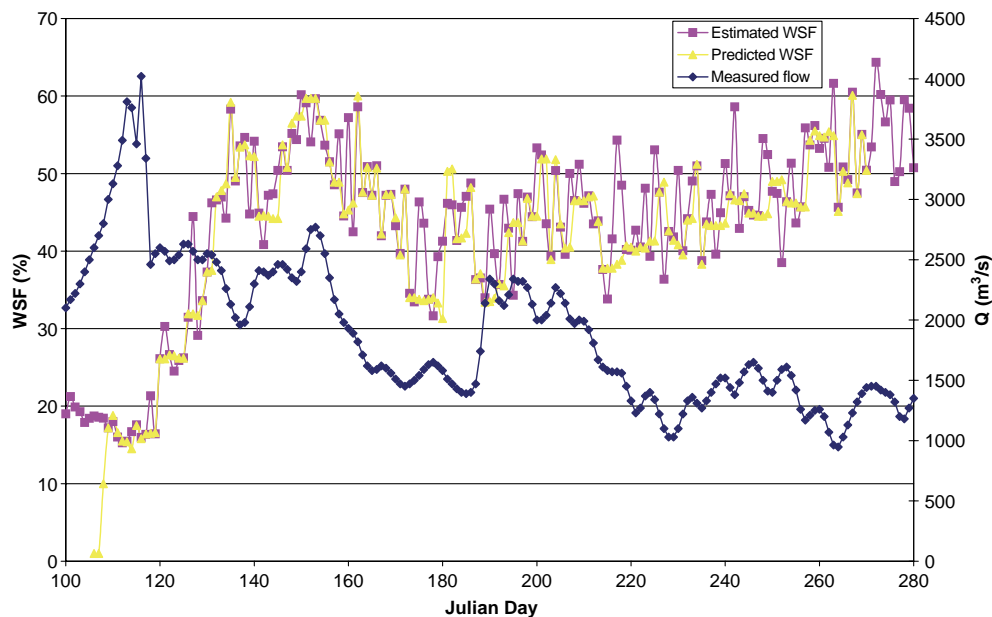

Fig. 6. Predicted and estimated WSF compared to the Peace River discharge, over the PAD, during the summer of 1998.
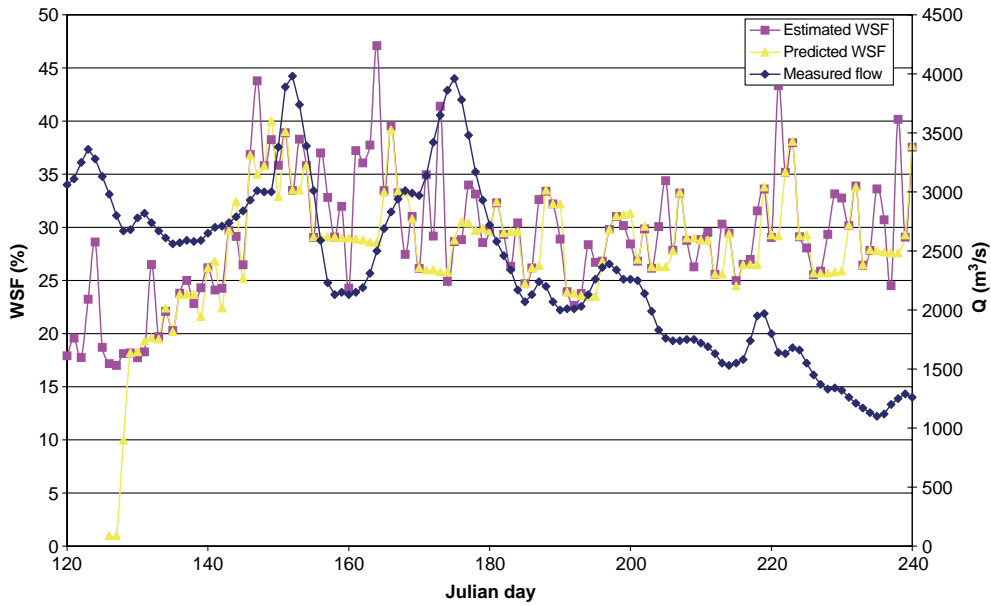
Fig. 7. Predicted and estimated WSF compared to the Peace River discharge, over the PAD, during the summer of 1999.

(Kochtubajda et al., 2000). The EL Nino phenomenon was observed during this year (Rouse, 2000).

Moreover, a perfect synchronism between the estimated and predicted WSF can be obtained as a result of the introduction of the time lag. Although the predicted WSFs are generated from the discharge data, which does not necessarily coincide with the estimated water surface extent, the dynamic rating curve model was nonetheless able to eliminate this lag and synchronize the estimated and predicted WSF. The time lag parameter is estimated on a daily basis using the ten last discharge and WSF observations. The absolute values of the obtained time lag vary between 0 and 7 days in the PAD case study. It was expected that this parameter would be of no

more than a few days due to the small size of the PAD area (4000 km^2) and the close location of the flow observation station over the Slave River to the PAD area.

In order to assess the reliability of the proposed approach, WSF maps were generated using NOAA-AVHRR images taken over the Mackenzie River Basin during the summers of 1998 and 1999. Three channels (channel $1 : 0.58-0.68$ μ, channel $2 : 0.72-1.10$ μ and channel $3 : 3.55-3.93$ μ) were classified in order to identify the WSF extent. The Peace Athabasca Delta site was selected for the validation process. Fig. 8 constitutes an example of the NOAA images taken over the selected site. Available NOAA-AVHRR images were examined, and those that
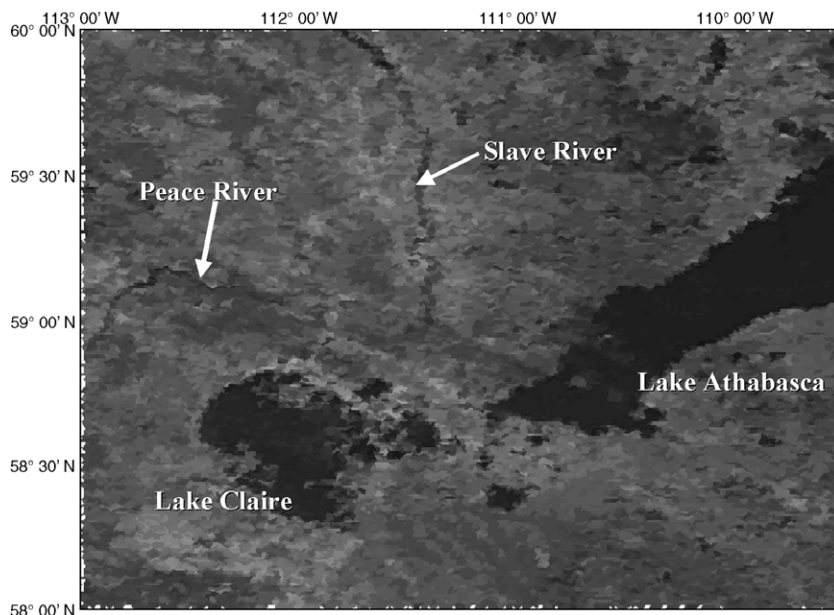

Fig. 8. NOAA-AVHRR image of the PAD, August 24th, 1999.
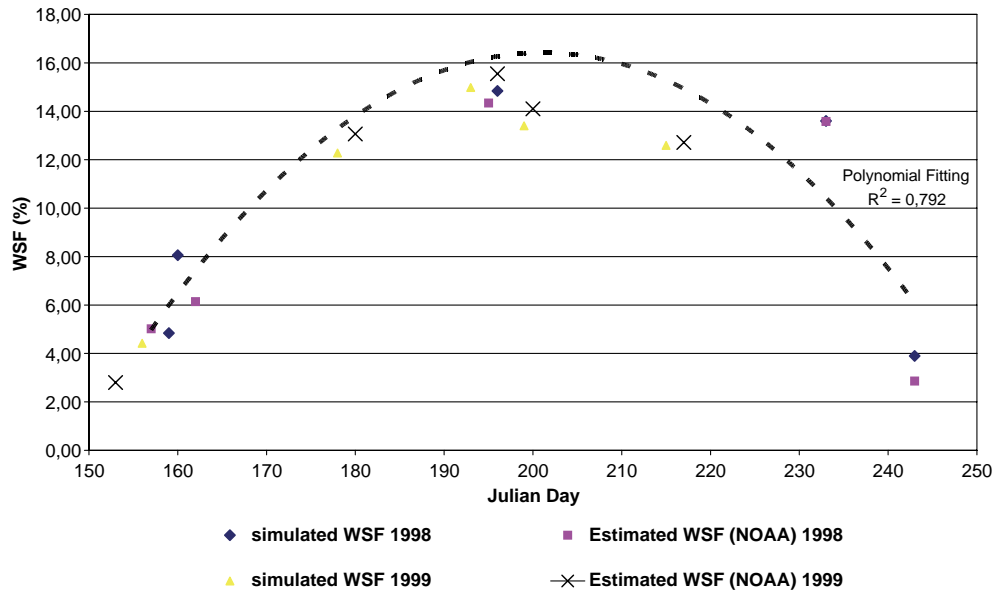
Fig. 9. Predicted WSF compared to those estimated from NOAA-AVHRR images, over the PAD, during the summers of 1999 and 1998.

were cloud-free were retained for analysis. WSFs were derived from NOAA-AVHRR and SSM/I data covering the same region, which is little larger than that used previously with SSM/I data in order to improve the classification performance. The results of the comparison are shown in Fig. 9. A satisfactory agreement can be observed between the WSF estimated from NOAA-AVHRR images and those predicted by the modified rating curve model. Both of them follow the general trend described above for the WSF evolution over the Mackenzie River Basin. However, an abrupt decrease was observed during the 1998 summer season. WSF seemed to be underestimated during this period of the year.

Although, the reliability of this approach has been tested over two delta sites, its applicability over the entire Mackenzie River Basin should be assessed in further studies, which will be our goal in future works. On the other hand, considering that only the spring and summer periods were examined in this study, it was assumed that the contribution of ice thawing to inundation is larger than that of precipitation during this period in the MRB (Marsh & Hey, 1989). This implies a larger correlation between discharge and flooded areas, which improves the potential of the proposed approach in sub-artic regions.

3.3. Use of passive microwave data for discharge forecasting

The existing correlation between discharge and WSF can also be used to predict discharge values particularly in case of positive time lag when the peak flow occurs after the peak flooded area. In this particular case the discharge can be written as:

$$Q = a.\text{WSF}^b(t + \text{d}.\Delta\text{t}) \qquad (11)$$

The proposed algorithm can, therefore, be applied to predict discharge values in an upstream location. The empirical parameters and the time lag term are dynamically readjusted as it was previously discussed. The availability of discharge observations and passive microwave data has enabled us to extend simulations beyond the two years, 1998 and 1999. The flow observed over the Slave River, which is located at 59°52 N, 111°35 W (Fig. 1), was used in combination with SSM/I measurements over the PAD from 1992 to 2000. Only summer periods were considered in carrying out simulations. WSF values were used to predict the flow over the Slave River Site because of the downstream location of the discharge observing station.

A predefined regression relationship between flooded areas and discharges is not needed in this case to extend the record of the flooded area as the use of the Kalman filter allows the readjustment of the rating parameters dynamically. Fig. 10 shows the simulation results. The predicted and observed discharge values were averaged on a weekly basis. A satisfactory agreement was observed between the predicted and observed discharge. Moreover, this figure demonstrates an apparent interannual variability of the discharge over Slave River observing station. From 1992 to 2000, the PAD area drained by the Slave River was fluctuating between wet and dry years. The 1995/1996 water year seems to be the beginning of a wetting phase of the delta, which ended during the summer of 1998, which coincides with an EL Nino phenomenon, with an abnormally high temperatures. Leconte et al. (2001) stated that 1996 seems to be one of the wettest years on record. On the other hand, an abnormally low discharge was observed during the 1994/95 water year (Strong et al., 2002) which corroborates the predicted discharge.

These simulations show again that the time lag parameter varies in absolute value between 0 and 7 days, when WSF is
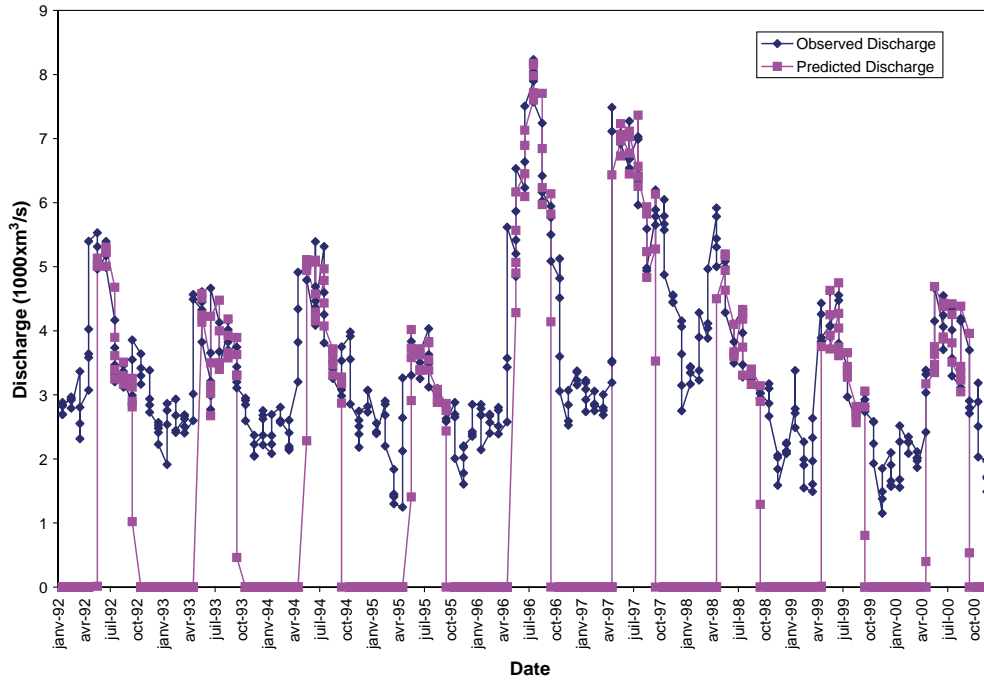
Fig. 10. Predicted and observed discharge over the Slave River observing station from 1992 to 2000.

estimated over the PAD and discharge is observed over the Slave River. However, this parameter does not show a significant interannual variability as its annual average (Fig. 11) varies slightly, at approximately two days. An average surface flow speed of 0.6 m/s (Louie et al., 2002) and a time lag value of 2.5 days lead to a runoff distance of 130 km that is compatible with the actual drainage distance between the discharge observation station over the Slave River and the PAD area, which is about 100 km.

It is worth mentioning that the dynamic readjustment of the parameters of the model offers a satisfactory flexibility to the model and enables its use either for flood or flow forecasting, as was tested previously (Smith et al., 1996). In these two cases, the Kalman filter dynamically readjusts the model parameters upon the reception of each new satellite image. The daily availability of the passive microwave data is very important for the application of the proposed approach.
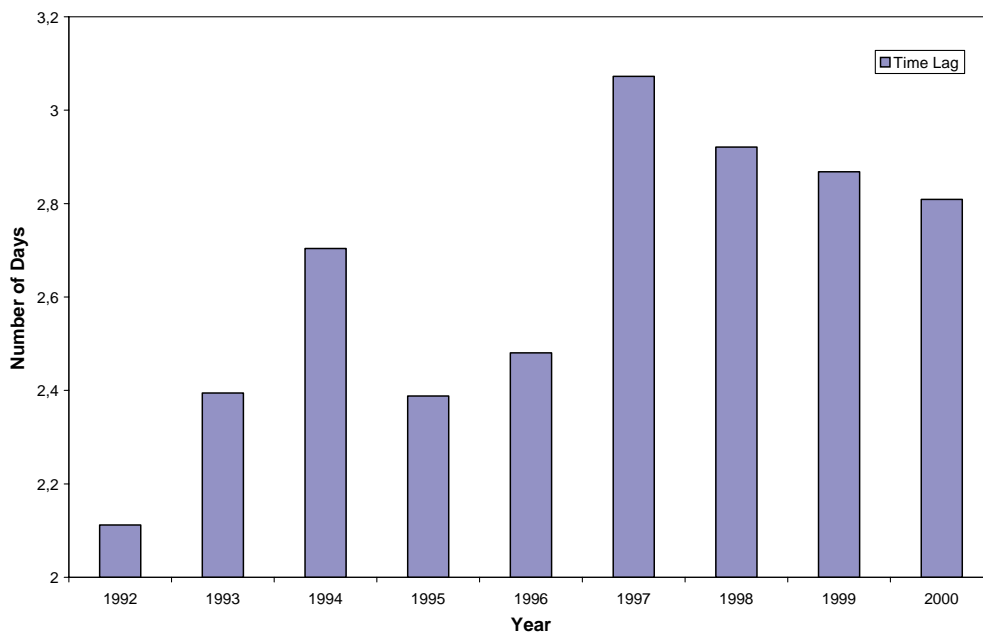

Fig. 11. Variability of the averaged time lag parameter from 1992 to 2000 over the PAD area.

4. Conclusion

In northern climates, ice jamming complicates the flooding process, causing it to evolve rapidly, and causing considerable economic and social damage. Hence, flood forecasting over this area is of great importance. The aim of this work is to provide a real-time forecasting of the water surface extent over two control sites selected from the Mackenzie River Basin using passive microwave data and discharge observations. The proposed methodology is based on the rating curve model, which was modified, by having a lag term introduced into its classical formulation. This lag term is responsible for a lag time observed between the WSF and discharge peaks. The modified rating curve model was coupled with the Kalman filter to update the empirical parameters of the model upon the reception of each new SSM/I image. The modified model is flexible and adapted to variable morphological features. Furthermore, the proposed approach makes it possible to overcome the site dependency of the rating curve model. The reliability of the approach was tested over the Peace Athabasca Delta, PAD and the Mackenzie River Delta, MRD. The WSF, estimated using NOAA-AVHRR images, were compared to those predicted over the PAD control site using SSM/I passive microwave data. The WSF from NOAA-AVHRR images fit the predicted values reasonably well. Satisfactory results were also obtained from the summers of 1992 to 2000 despite an interannual variability of both discharge and flooded areas. This implies that a combination of passive microwave data and discharge data presents an interesting potential in flood and discharge prediction.

References

Armstrong, R., Knowles, K., Brodzik, M., & Hardman, M. (1994). *DMSP SSM/I Pathfinder daily EASE-Grid brightness temperatures*. Boulder, CO: National Snow and Ice Data Center.

Basist, A., Grody, N. C., Peterson, T. C., & Williams, C. N. (1998). Using the special sensor microwave/imager to monitor land surface temperatures, wetness, and snow cover. *Journal of Applied Meteorology*, *37*(9), 888–911.

Basist, A., Williams, C., Grody, N., Ross, T. F., Shen, S., Chang, A. T. C., et al. (2001). Using the special sensor microwave imager to monitor surface wetness. *Journal of Hydrometeorology*, *2*(3), 297–308.

Burn, C. R. (1995). Hydrologic regime of Mackenzie River and connection of 'no-closure' lakes to distributary channels in the Mackenzie Delta, Northwest territories. *Canadian Journal of Earth Sciences*, *32*(7), 926–937.

Fily, M., Royer, A., Goita, K., & Prigent, C. (2003). A simple retrieval method for land surface temperature and fraction of water surface determination from satellite microwave brightness temperatures in subarctic areas. *Remote Sensing of Environment*, *85*(3), 328–338.

Frazier, P., Page, K., Louis, J., Briggs, S., & Robertson, A. I. (2003). Relating wetland inundation to river flow using Landsat TM data. *International Journal of Remote Sensing*, *24*(19), 3755–3770.

Jin, Y. -Q. (1999). Flooding index and its regional threshold value for monitoring floods in China from SSM/I data. *International Journal of Remote Sensing*, *20*(5), 1025–1030.

Kerr, Y. H., & Njoku, E. G. (1993). On the use of passive microwaves at 37 GHz in remote sensing of vegetation. *International Journal of Remote Sensing*, *14*(10), 1931–1943.

Kochtubajda, B., Stewart, R. E., Gyakum, J. R., & Flannigan, M. D. (2000). Convection, lightning and fire disturbances in the Mackenzie River Basin. *6th Scientific workshop for MAGS*.

Kruus, J., Deutsch, M., Hansen, P. L., & Ferguson, H. L. (1981). Flood application of satellite imagery. *Fifth Annual William T. Pecora Memorial Symposium on remote sensing, 1979*.

Leconte, R., Pietroniro, A., Peters, D. L., & Prowse, T. D. (2001). Effects of flow regulation on hydrologic patterns of a large, inland delta. *Regulated Rivers: Research and Management*, *17*(1), 51–65.

Louie, P. Y. T., Hogg, W. D., MacKay, M. D., Zhang, X., & Hopkinson, R. F. (2002). The water balance climatology of the Mackenzie basin with reference to the 1994/95 water year. *Atmosphere-Ocean*, *40*(2), 159–180.

MacKay, M. D., Seglenieks, F., Verseghy, D., Soulis, E. D., Snelgrove, K. R., Walker, A., et al. (2003). Modeling Mackenzie basin surface water balance during CAGES with the Canadian regional climate model. *Journal of Hydrometeorology*, *4*(4), 748–767.

Marsh, P., & Hey, M. (1989). The flooding hydrology of Mackenzie Delta Lakes near Inuvik, N.W.T., Canada. *Arctic*, *42*, 41–49.

Mosley, M. P. (1983). Response of braided rivers to changing discharge. *Journal of Hydrology*, *22*(1), 18–67.

Rouse, W. R. (2000). Progress in hydrological research in the Mackenzie GEWEX study. *Hydrological Processes*, *14*(9), 1667–1685.

Sippel, S. J., Hamilton, S. K., Melack, J. M., & Choudhury, B. J. (1992). Inundation area and morphometry of lakes on the Amazon River floodplain, Brasil. *Archiv für Hydrobiologie*, *123*, 385–400.

Sippel, S. J., Hamilton, S. K., Melack, J. M., & Novo, E. M. M. (1998). Passive microwave observations of inundation area and the area/stage relation in the Amazon River floodplain. *International Journal of Remote Sensing*, *19*(16), 3055–3074.

Smith, L. C., Isacks, B. L., & Bloom, A. L. (1996). Estimation of discharge from three braided rivers using synthetic aperture radar satellite imagery: Potential application to ungaged basins. *Water Resources Research*, *32*(7), 2021–2034.

Smith, L. C., Isacks, B. L., Forster, R. R., Bloom, A. L., & Preuss, I. (1995). Estimation of discharge from braided glacial rivers using ERS 1 synthetic aperture radar: First results. *Water Resources Research*, *31*(5), 1325–1329.

Stewart, R. E., Leighton, H. G., Marsh, P., Moore, G. W. K., Ritchie, H., Rouse, W. R., et al. (1998). The Mackenzie GEWEX Study: The water and energy cycles of a major North American river basin. *Bulletin of the American Meteorological Society*, *79*(12), 2665–2683.

Strong, G. S., Proctor, B., Wang, M., Soulis, E. D., Smith, C. D., Seglenieks, F., et al. (2002). Closing the Mackenzie Basin water budget, water years 1994/95 to 1996/97. *Atmosphere-Ocean*, *40*(2), 113–124.

Tanaka, M., Sugimura, T., Tanaka, S., & Tamai, N. (2003). Flood-drought cycle of Tonle Sap and Mekong Delta area observed by DMSP-SSM/I. *International Journal of Remote Sensing*, *24*(7), 1487–1504.

Toyra, J., Pietroniro, A., Martz, L. W., & Prowse, T. D. (2002). A multi-sensor approach to wetland flood monitoring. *Hydrological Processes*, *16*(8), 1569–1581.

Vorosmarty, C. J., Willmott, C. J., Choudhury, B. J., Schloss, A. L., Steams, T. K., Robeson, S. M., et al. (1996). Analyzing the discharge regime of a large tropical river through remote sensing, ground-based climatic data, and modeling (Paper 96WR01333). *Water Resources Research*, *32*(10), 3137–3150.

Williams, C. N., Basist, A., Peterson, T. C., & Grody, N. (2000). Calibration and verification of land surface temperature anomalies derived from the SSM/I. *Bulletin of the American Meteorological Society*, *81*(9), 2141–2156.